

# The observational constraints on the flat $\phi$ CDM models.

Olga Avsajanishvili,<sup>1</sup> Yiwen Huang,<sup>2</sup> Lado Samushia,<sup>3,1</sup> and Tina Kahniashvili<sup>2,4,1</sup>

<sup>1</sup>*Abastumani Astrophysical Observatory, Ilia State University, 3-5 Cholokashvili Ave., Tbilisi, 0194, Georgia*

<sup>2</sup>*McWilliams Center for Cosmology and Department of Physics,  
Carnegie Mellon University, 5000 Forbes Ave, Pittsburgh, PA 15213 USA*

<sup>3</sup>*Department of Physics, Kansas State University,  
116 Cardwell Hall, Manhattan, KS, 66506, USA*

<sup>4</sup>*Department of Physics, Laurentian, University, Ramsey Lake Road, Sudbury, ON P3E 2C, Canada*

(Dated: November 27, 2018)

Current cosmological data is in a good agreement with the  $\Lambda$ CDM model as well as a number of physically better motivated alternatives. The constraining power of the cosmological data is steadily increasing and if the standard cosmological *concordance* ( $\Lambda$ CDM) model is not a true description of dark energy we will be able to reject it within the next decade. If however the  $\Lambda$ CDM model (or something effectively very close to the  $\Lambda$ CDM model) constitutes the true nature of dark energy the statistical interpretation of the result will not be as straightforward. Most dark energy models have the  $\Lambda$ CDM model as their limit and the Bayesian arguments about evidence and the fine-tuning will have to be employed to discriminate between the models. Assuming a baseline  $\Lambda$ CDM model we look at a number of the representative dark energy models would perform when compared to the growth rate, the expansion rate, and the angular distance measurements from the Stage-IV dark energy experiments. We find that the Bayes factor will provide a substantial evidence in favor of the  $\Lambda$ CDM model over most of the alternatives.

## I. INTRODUCTION

It is well established that our universe is undergoing an accelerating expansion today [1–3]. Several observations suggest that this accelerated expansion started relatively recently at  $z \sim 0.7$  [4, 5]. One of the possible explanations of the late time accelerated expansion is to assume the presence of dark energy as a dominant component in the universe’s total energy density budget today (i.e. around 70% of the today universe matter-energy content is a substance with the negative pressure that insures today’s accelerated expansion). Dark energy is characterized by an equation of state (EOS) parameter  $w < -1/3$ . In the framework of the  $\Lambda$ CDM model dark energy is represented by the cosmological constant. The  $\Lambda$ CDM model is simple and easy to constrain with observational data but has a number of shortcomings (the cosmological constant problem, the coincidence problem, the matter - anti-matter asymmetry, the weakness of gravity compared to other forces, etc.) [6–9]. Most notable of these is the cosmological constant problem which stems from the fact that the theoretically expected energy density of cosmological constant is of order of  $M_{\text{Pl}}^4$  (where  $M_{\text{Pl}}$  is the Planck mass), while the actual value is 120 magnitudes lower [10–12]. In order to overcome these (and other) difficulties, the *dynamical* dark energy models were proposed [13].

In this paper we investigate a representative family of the dark energy models that are based on the idea of a cosmological scalar field [14–20]. If the scalar field  $\phi$  has a slowly rolling stage it can mimic the behavior of the cosmological constant. There are many proposals for the functional form of the self-interacting potential of the scalar field that are allowed by the current data [14, 17, 18, 21–31]. In this paper we consider two types of scalar field dark energy models: the quintessence and the phantom models. As of now, there is no consensus on which of these models is preferable based on the results obtained from the different observational data [32–35]. We have studied the models with 10 quintessence and 7 phantom potentials in Bayesian framework [36–38]. We have compared these models with a baseline  $\Lambda$ CDM model. We have found that if the cosmological constant is the correct description of dark energy (despite the problem associated with its value), a vast majority of the dynamical dark energy models will be characterized by low enough Bayes factors to suggest a substantial preference for the  $\Lambda$ CDM model.

Several Stage-IV experiments, such as e.g. Dark Energy Spectroscopic Instrument (DESI), Dark Energy Survey (DES), Wide-Field Infrared Survey Telescope (WFIRST) and Euclid are scheduled to start operating within the next decade. Once these missions are completed we will have very accurate measurements of the expansion rate, the growth rate, and the angular distance of the universe up to the redshifts of  $z \sim 2.0$  [39–44]. If the  $\Lambda$ CDM model is *not* the correct cosmological model, we will be able to see this in data. If, however, the  $\Lambda$ CDM model or something very close to it is the correct model, the interpretation of the data will be less straightforward. One reason for this is that the most viable dark energy models have the  $\Lambda$ CDM model as their limit so the Bayesian arguments about the fine-tuning of the extra parameters will have to be employed. We take a baseline the  $\Lambda$ CDM model and study how these models would perform in the light of data from DESI.

DESI is expected to measure the angular distance, the Hubble parameter, and the growth rate of the structure over a wide range of the redshifts up to  $z = 2.0$ . These measurements cumulatively have a very strong constraining power on the behavior of both dark energy and gravity on large length scales [39–41].

The paper is organized as follows: in Sec. II we review the dark energy models (including the scalar field quintessence and phantom models); in Sec. III we describe observational tests, our results are presented in Sec. IV, and we conclude in Sec. V. We use natural units:  $c = \hbar = k_B = 1$  throughout the paper.

## II. DARK ENERGY MODELS

In the scalar field models, dark energy is presented in the form of a slowly varying cosmological homogeneous scalar field  $\phi$ , and the corresponding cosmological model is called  $\phi$ CDM model. We will consider two families of the scalar field dark energy models: the quintessence and the phantom scalar field models. These models have opposite properties in their manifestation today: in the range of the EOS parameter values ( $w_\phi < -1$  for the phantom field and  $-1/3 < w_\phi < -1$  for the quintessence field); in the sign of the kinetic term in the Lagrangian (the negative sign for the phantom field and the positive one for the quintessence field); in the dynamics of the scalar fields (the quintessence field rolls to the minimum its potential, the phantom field rolls to the "uphill" its potential), in the dynamics of the dark energy density (increases over time for the phantom field and almost doesn't change over time for the quintessence field); in the forecast for the future evolution of the universe (the disintegration or rip (big/little/pseudo) of the universe will occur for the phantom field and the eternal "mild" expansion in the case of the flat/open universe and re-collapsing in the case of the close universe for the quintessence field).

The scalar  $\phi$  field dark energy models are described by the action

$$S = \frac{M_{\text{pl}}^2}{16\pi} \int d^4x \left[ \sqrt{-g} \left( \pm \frac{1}{2} g^{\mu\nu} \partial_\mu \phi \partial_\nu \phi - V(\phi) \right) \right], \quad (1)$$

where "+" sign before the kinetic term refers to the quintessence models, while "-" stands for the phantom models;  $g^{\mu\nu}$  is the background metric,<sup>1</sup> and  $V(\phi)$  is the self-interacting potential of the scalar field. The scalar field is assumed to exhibit negligible spatial variations, so that the spatial derivatives are small compared to the time derivatives.

Varying the action Eq. (1), the dynamical equation for the scalar field is

$$\ddot{\phi} + 3\frac{\dot{a}}{a}\dot{\phi} \pm \frac{\partial V(\phi)}{\partial \phi} = 0, \quad (2)$$

where again "+/-" sign corresponds to the quintessence/phantom model respectively, the over-dot denotes a derivative with respect to physical time  $t$ .

The energy density and the pressure of the scalar field are

$$\rho_\phi = \frac{M_{\text{pl}}^2}{32\pi} \left( \pm \dot{\phi}^2/2 + V(\phi) \right), \quad (3)$$

$$P_\phi = \frac{M_{\text{pl}}^2}{32\pi} \left( \pm \dot{\phi}^2/2 - V(\phi) \right), \quad (4)$$

and the effective EOS parameter for the scalar field is then given by  $w_\phi = \frac{\pm \dot{\phi}^2/2 - V(\phi)}{\pm \dot{\phi}^2/2 + V(\phi)}$ . If the time-derivatives

of the scalar field  $\phi$  are small enough to make the magnitude of the kinetic term small compared to the potential  $|\pm \dot{\phi}^2/2| \ll V(\phi)$  (the "slow roll" condition), the EOS parameter is very close to negative one and the scalar field behaves like a time-varying cosmological constant.<sup>2</sup> Below we list the quintessential and phantom models potentials considered in this work:

<sup>1</sup> We assume the flat (suggested by current observations [35]), homogeneous and isotropic universe that is described by the Friedmann-Lemaître-Robertson-Walker (FLRW) spacetime metric,  $ds^2 = dt^2 - a^2(t)d\mathbf{x}^2$ , where  $a(t)$  is the scalar factor (normalized to be unity today  $a_0 \equiv a(t_0)$ ), and  $t$  is the physical time.

<sup>2</sup> More precisely, for the freezing quintessence scalar fields the EOS parameter is very close to negative one today, while for the thawing quintessence/phantom scalar fields the EOS parameter deviates slightly from minus one in either direction.

### 1. The quintessence models

- Ratra-Peebles (RP) potential:  $V(\phi) = V_0 M_{\text{pl}}^2 \phi^{-\alpha}$ ;  $\alpha = \text{const} > 0$  [14]
- Ferreira-Joyce potential  $V(\phi) = V_0 \exp(-\lambda\phi/M_{\text{pl}})$ ;  $\lambda = \text{const} > 0$  [21]
- Sugra potential:  $V(\phi) = V_0 \phi^{-\chi} \exp(\gamma\phi^2/M_{\text{pl}}^2)$ ;  $\chi, \gamma = \text{const} > 0$  [22]
- Inverse exponent potential:  $V(\phi) = V_0 \exp(M_{\text{pl}}/\phi)$  [18]
- Zlatev-Wang-Steinhardt (ZWS) potential:  $V(\phi) = V_0 (\exp(M_{\text{pl}}/\phi) - 1)$  [17]
- Sahni-Wang potential:  $V(\phi) = V_0 (\cosh(\zeta\phi) - 1)^g$ ;  $\zeta = \text{const} > 0$ ,  $g = \text{const} < 1/2$  [23]
- Ur̄ena-López-Matos potential:  $V(\phi) = V_0 \sinh^m(\xi M_{\text{pl}}\phi)$ ;  $\xi = \text{const} > 0$ ,  $m = \text{const} < 0$  [24]
- Albrecht-Skordis potential:  $V(\phi) = V_0 ((\phi - B)^2 + A) \exp(-\mu\phi)$ ;  $A, B = \text{const} \geq 0$ ,  $\mu = \text{const} > 0$  [25]
- Chang-Scherrer potential:  $V(\phi) = V_0 (1 + \exp(-\tau\phi))$ ;  $\tau = \text{const} > 0$  [26]
- Barreiro-Copeland-Nunes potential:  $V(\phi) = V_0 (\exp(\nu\phi) + \exp(v\phi))$ ;  $\nu, v = \text{const} \geq 0$  [27]

### 2. The phantom models

- Quadratic potential :  $V(\phi) = V_0 \phi^2$  [28]
- Gaussian potential:  $V(\phi) = V_0 (1 - \exp(\phi^2/\sigma^2))$ ;  $\sigma = \text{const}$  [28]
- Pseudo Nambu-Goldstone boson (pNGb) potential:  $V(\phi) = V_0 (1 - \cos(\phi/\kappa))$ ;  $\kappa = \text{const} > 0$  [29]
- Inverse hyperbolic cosine potential:  $V(\phi) = V_0 (\cosh(\psi\phi))^{-1}$ ;  $\psi = \text{const} > 0$  [30]
- Fifth power potential:  $V(\phi) = V_0 \phi^5$  [31]
- Inverse quadratic potential:  $V(\phi) = V_0 \phi^{-2}$  [31]
- Exponent potential:  $V(\phi) = V_0 \exp(\beta\phi)$ ;  $\beta = \text{const} > 0$  [31]

In both cases  $V_0$  is the model parameter with the dimensions of  $\text{GeV}^4$ .

## III. TESTING DARK ENERGY POTENTIALS

### A. The basic equations

To see how well we will be able to discriminate between these dark energy scalar field potentials after Stage-IV data we generate a set of the measurements of the growth rate, the Hubble expansion rate, and the angular distance in the redshift range of  $0.15 < z < 1.85$  expected from DESI mission [39] ( $z = 1/a - 1$  is the redshift). The measurements are centered around their true values in our fiducial cosmology with the errorbars based on the Fisher matrix predictions. We then run Markov Chain Monte Carlo (MCMC) for each dark energy potential to get the multidimensional posterior likelihood. We fit this synthetic data by using the standard MCMC analysis method to estimate the posterior likelihood of the model parameters.

For all dark energy models we compute:

i) The Hubble parameter  $H(z)$ .

The first Friedmann equation for the flat universe is

$$E^2(z) = \Omega_{r,0}(1+z)^4 + \Omega_{m,0}(1+z)^3 + \Omega_\phi(z), \quad (5)$$

here  $E(z) = H(z)/H_0$  is the normalized Hubble parameter, and  $H_0$  is the Hubble parameter today.  $\Omega_i(z)$  is the energy density parameter for i-component with the energy density  $\rho_i$ ,<sup>3</sup>

ii) The angular distance:

$$d_A(z) = \frac{1}{H_0(1+z)} \int_0^z \frac{dz'}{E(z')}. \quad (6)$$

---

<sup>3</sup> The energy density parameter  $\Omega_i(z)$  is defined as the ratio of  $\rho_i(z)$  to the critical energy density today  $\rho_{\text{cr}} = 3H_0^2(z)/(8\pi G)$ , where  $G = M_{\text{pl}}^{-2}$  is the Newton constant. Then, the current value of the radiation (relativistic component) and the matter (non-relativistic) density parameter are designated as  $\Omega_{r,0}$  and  $\Omega_{m,0}$  respectively;  $\Omega_\phi(z)$  is the dark energy density time dependent parameter.

iii) The combination of the growth rate and the power spectrum amplitude  $f\sigma_8(z)$ . The growth rate is defined as  $f = d\ln D/d\ln a$ ; the power spectrum amplitude is  $\sigma_8(z) = D\sigma_8$ ,  $\sigma_8 = \sigma_8(z=0)$ . The growth function  $D$  is a solution of the linear perturbation equation:

$$D'' + \left(\frac{3}{a} + \frac{E'}{E}\right)D' - \frac{3\Omega_{m,0}}{2a^5 E^2}D = 0, \quad (7)$$

here a prime denotes a derivative with respect to the scale factor  $a$ . We fix the value of  $\sigma_8$  to its current best-fit  $\Lambda$ CDM value of  $\sigma_8 = 0.815$  from large scale CMB experiments [35].

Dark energy is often described by the Chevallier-Polarsky-Linder (CPL)  $w_0 - w_a$  parametrization (so called  $w$ CDM) [45, 46]:

$$w_\phi = w_0 + w_a(1 - a), \quad (8)$$

where  $w_0 = w(a=1)$  and  $w_a = (dw/dz)|_{z=1}$ . This parametrization describes most of the dark energy models well enough for some effective values of  $w_0$  and  $w_a$ , but may fail to describe the arbitrary dark energy models to a good precision over a wide redshift range.

In addition, in the most dark energy models the growth of structure tends to be sensitive only to the fractional matter density  $\Omega_m(a) = \Omega_{m0}a^{-3}/E^2(a)$  and the growth rate of the matter perturbations  $f$  [47] to high accuracy can be parametrized as

$$f \approx [\Omega_m(a)]^{\gamma(a)}, \quad (9)$$

where  $\gamma(a)$  is a growth index. The numerical value of the  $\gamma(a)$  parameter itself depends on the dark energy model being equal to 0.55 for the  $\Lambda$ CDM model.

For the dark energy models that are well approximated by the  $w_0 - w_a$  parametrization, the evolution of the  $\gamma(a)$  function with its dependence on the scale factor can be determined from the Eq. (9) [48]:

$$\gamma(a) = \frac{\ln f}{\ln \Omega_m(a)}. \quad (10)$$

$\gamma(a)$  has a mild dependence on  $w_0$ ,  $w_a$  [49]

$$\gamma = \begin{cases} 0.55 + 0.05(1 + w_0 + 0.5w_a), & \text{if } w_0 \geq -1; \\ 0.55 + 0.02(1 + w_0 + 0.5w_a), & \text{if } w_0 < -1. \end{cases} \quad (11)$$

This parametrization is accurate up to redshift of  $z = 5$  [51].

In our work we also consider how well the  $w_0 - w_a$  parameters can describe the effective EOS parameter for the dynamic dark energy models. We find that for the models considered there is a set of  $w_0 - w_a$  that describes the effective background expansion and growth reasonably well.

To find the starting points for our MCMC chains we solve jointly the scalar field equation for the quintessence/phantom models Eq. (2) and the Friedmann equation Eq. (5) and after that the linear perturbation equation Eq. (7) for a wide range of the free parameters and the initial conditions for matter dominated epoch ( $\phi_0$ ,  $\dot{\phi}_0$ ). For each potential we have found the plausible solutions, for which the following three criteria were simultaneously fulfilled:

1. The transition between the matter and dark energy equality ( $\Omega_m = \Omega_\phi$ ) happens relatively recently  $z \in (0.6-0.8)$  [50].
2. the growth rate function  $f$  follows the  $\gamma$ -parametrization Eq. (11).
3. The EOS parameter predicted by the different dark energy models should be in the agreement with the expected EOS parameter value today (for the phantom models  $w_0 < -1$ ; for the freezing/thawing quintessence models:  $-1 < w_0 < -0.75$  and  $w_a < 0/w_a > 0$ ).

The RP potential has an attractor solution such that its late time evolution is identical for a wide range of initial conditions. For better numerical convergence we always choose initial conditions ( $\phi_0$ ,  $\dot{\phi}_0$ ), and the values  $V_0$  so that the solution lies on this attractor curve [50, 52, 53]

$$V_0 = \frac{8}{3} \left( \frac{\alpha + 4}{\alpha + 2} \right) \left[ \frac{2}{3} \alpha (\alpha + 2) \right]^{\alpha/2}, \quad (12)$$

$$\phi_0 = \left[ \frac{2}{3} \alpha (\alpha + 2) \right]^{1/2} a_{\text{in}}^{\frac{3}{\alpha+2}}, \quad (13)$$

$$\dot{\phi}_0 = \left[ \frac{8\alpha}{3(\alpha + 2)} \right]^{1/2} a_{\text{in}}^{-\frac{3\alpha}{2(\alpha+2)}}, \quad (14)$$

where the initial value of the scale factor  $a_{\text{in}}$  was set in matter dominated epoch. We applied the values of the model parameter  $\alpha \leq 0.7$ , which is accordance with current observational data [55].

For all potentials we have found the range of the initial conditions  $(\phi_0, \dot{\phi}_0)$  and the model parameters, which we then used as starting points for the MCMC chains.

## IV. RESULTS

### A. The Bayesian statistics

All dark energy models considered in this work have free parameters  $\Omega_{\text{m}}(z=0)$ ,  $H_0$ . The scalar field models have extra parameters describing the shape of the potential and the initial conditions. These free parameters along with prior ranges considered in our MCMC runs are presented in the Tables I and II.

The quintessence potentials	Free parameters
$V(\phi) = V_0 M_{\text{pl}}^2 \phi^{-\alpha}$	$V_0(3 - 5), \alpha(10^{-6} - 0.7), H_0(65 - 73), \Omega_{\text{m}0}(0.25 - 0.32)$
$V(\phi) = V_0 \exp(-\lambda\phi/M_{\text{pl}})$	$V_0(10 - 10^3), \lambda(10^{-7} - 10^{-3}), H_0(65 - 73), \Omega_{\text{m}0}(0.25 - 0.32), \phi_0(0.2 - 1.6), \dot{\phi}_0(79.8 - 338.9)$
$V(\phi) = V_0 \phi^{-x} \exp(\gamma\phi^2/M_{\text{pl}}^2)$	$V_0(10^{-2} - 10^{-1}), \chi(4 - 8), \gamma(6.5 - 7), H_0(65 - 73), \Omega_{\text{m}0}(0.25 - 0.32), \phi_0(5.78 - 10.55), \dot{\phi}_0(680.6 - 879)$
$V(\phi) = V_0 \exp(M_{\text{pl}}/\phi)$	$V_0(10^2 - 10^3), H_0(65 - 73), \Omega_{\text{m}0}(0.25 - 0.32), \phi_0(5.78 - 10.55), \dot{\phi}_0(680.6 - 879)$
$V(\phi) = V_0(\exp(M_{\text{pl}}/\phi) - 1)$	$V_0(10 - 10^2), H_0(65 - 73), \Omega_{\text{m}0}(0.25 - 0.32), \phi_0(1.5 - 10), \dot{\phi}_0(350 - 850)$
$V(\phi) = V_0(\cosh(\zeta\phi) - 1)^g$	$V_0(5 - 8), \zeta(0.15 - 1), g(0.1 - 0.49), H_0(65 - 73), \Omega_{\text{m}0}(0.25 - 0.32), \phi_0(1.8 - 5.8), \dot{\phi}_0(360 - 685)$
$V(\phi) = V_0 \sinh^m(\xi M_{\text{pl}}\phi)$	$V_0(1 - 10), m(-0.1 - -0.3), \xi(10^{-2} - 1), H_0(65 - 73), \Omega_{\text{m}0}(0.25 - 0.32), \phi_0(0.5 - 2.5), \dot{\phi}_0(190 - 367)$
$V(\phi) = V_0((\phi - B)^2 + A) \exp(-\mu\phi)$	$V_0(40 - 70), A(1 - 40), B(1 - 60), \mu(0.2 - 0.9), H_0(65 - 73), \Omega_{\text{m}0}(0.25 - 0.32), \phi_0(5.8 - 8.45), \dot{\phi}_0(681 - 804.5)$
$V(\phi) = V_0(1 + \exp(-\tau\phi))$	$V_0(1 - 10^2), \tau(10 - 10^2), H_0(65 - 73), \Omega_{\text{m}0}(0.25 - 0.32), \phi_0(0.01 - 0.075), \dot{\phi}_0(9.4 - 32)$
$V(\phi) = V_0(\exp(\nu\phi) + \exp(\nu\phi))$	$V_0(1 - 12), \nu(6 - 12), H_0(65 - 73), \Omega_{\text{m}0}(0.25 - 0.32), \phi_0(0.014 - 1.4), \dot{\phi}_0(9.4 - 311)$

TABLE I: The list of the dark energy quintessence potentials and the free parameters.

The phantom potentials	Free parameters
$V(\phi) = V_0 \phi^2$	$V_0(1 - 20), H_0(65 - 73), \Omega_{\text{m}0}(0.25 - 0.32), \phi_0(0.67 - 2.8), \dot{\phi}_0(191 - 450)$
$V(\phi) = V_0(1 - \exp(\phi^2/\sigma^2))$	$V_0(5 - 30), \sigma(5 - 30), H_0(65 - 73), \Omega_{\text{m}0}(0.25 - 0.32), \phi_0(0.67 - 2.8), \dot{\phi}_0(191 - 450)$
$V(\phi) = V_0(1 - \cos(\phi/\kappa))$	$V_0(1 - 4), \kappa(1.1 - 2), H_0(65 - 73), \Omega_{\text{m}0}(0.25 - 0.32), \phi_0(2.3 - 3.37), \dot{\phi}_0(420 - 500)$
$V(\phi) = V_0(\cosh(\psi\phi))^{-1}$	$V_0(10^{-3} - 10^2), \psi(10^{-3} - 1), H_0(65 - 73), \Omega_{\text{m}0}(0.25 - 0.32), \phi_0(1.4 - 2.3), \dot{\phi}_0(310 - 420.7)$
$V(\phi) = V_0 \phi^5$	$V_0(10^{-3} - 10^{-2}), H_0(65 - 73), \Omega_{\text{m}0}(0.25 - 0.32), \phi_0(3.37 - 3.94), \dot{\phi}_0(523 - 563.6)$
$V(\phi) = V_0 \phi^{-2}$	$V_0(30 - 50), H_0(65 - 73), \Omega_{\text{m}0}(0.25 - 0.32), \phi_0(2.83 - 5.15), \dot{\phi}_0(471.4 - 600)$
$V(\phi) = V_0 \exp(\beta\phi)$	$V_0(1 - 20), \beta(0.08 - 0.3), H_0(65 - 73), \Omega_{\text{m}0}(0.25 - 0.32), \phi_0(0.2 - 9.14), \dot{\phi}_0(79.8 - 830.9)$

TABLE II: The list of the dark energy phantom potentials and the free parameters.

These priors we got using the phenomenological method, describing in the previous section, i.e. they satisfy by the three conditions imposed on the solutions obtained for each potential. Outside the ranges of the found priors, these

three conditions are not fulfilled at the same time. These priors do not otherwise include any additional insight or naturalness arguments.

To assess the quality of the different models and to distinguish them from each other, we have applied the Akaike information criterion (*AIC*) [54] and the Bayesian (or Schwarz) information criterion (*BIC*) [56]. The information obtained by these criteria complement each other.

*AIC* and *BIC* are defined respectively as

$$AIC = -2 \ln \mathcal{L}_{max} + 2k, \quad (15)$$

and

$$BIC = -2 \ln \mathcal{L}_{max} + k \ln N, \quad (16)$$

where  $\mathcal{L}_{max} \propto \exp(-\chi_{min}^2/2)$  is a maximum value of the likelihood function;  $N$  is the number of free parameters;  $k$  is number of data points.

We also computed the evidence integral defined as

$$\mathcal{E} = \int d^3 \mathbf{p} \mathcal{P}(\mathbf{p}), \quad (17)$$

where  $\mathbf{p}$  are all parameters of the model and the boundaries of the integral are given by the prior. We explored how tight the prior on the extra parameters needs to be for them to be competitive (in the sense of the Bayesian evidence) with the standard  $\Lambda$ CDM model.

We explicitly checked that the priors incorporate most of the high posterior area. Since all dark energy models have the  $\Lambda$ CDM model as their limit, ruling them out simply based on the posterior is technically speaking impossible. One could however appeal to the Bayesian evidence and argue that the extra parameters need to be extremely fine tuned. We numerically integrated the posterior likelihood to get for all models.

These results are presented in the Tables III and IV.

The quintessence potentials	BIC	AIC	Bayes factor
$V(\phi) = V_0 M_{pl}^2 \phi^{-\alpha}$	18.7	10	0.016
$V(\phi) = V_0 \exp(-\lambda \phi / M_{pl})$	22.4	12	0.0026
$V(\phi) = V_0 \phi^{-\chi} \exp(\gamma \phi^2 / M_{pl}^2)$	26.2	14	0.0012
$V(\phi) = V_0 \exp(M_{pl} / \phi)$	18.7	10	0.056
$V(\phi) = V_0 (\exp(M_{pl} / \phi) - 1)$	18.7	10	0.017
$V(\phi) = V_0 (\cosh(\zeta \phi) - 1)^g$	26.2	14	0.0013
$V(\phi) = V_0 \sinh^m(\xi M_{pl} \phi)$	26.2	14	0.0034
$V(\phi) = V_0 ((\phi - B)^2 + A) \exp(-\mu \phi)$	29.9	16	0.0059
$V(\phi) = V_0 (1 + \exp(-\tau \phi))$	22.4	12	0.0016
$V(\phi) = V_0 (\exp(\nu \phi) + \exp(v \phi))$	26.2	14	0.0035

TABLE III: The list of the dark energy quintessence potentials, with corresponding *BIC*, *AIC*, and Bayes factors.

All these numbers are normalized with respect to the fiducial  $\Lambda$ CDM model.

## B. The $\phi$ CDM potentials vs CPL parametrization

In order to check how well the CPL parametrization Eq. (8) describes the dark energy models we find the best-fit effective values of  $w_0 - w_a$  for a range of free parameters of the model. These results are presented in Fig. (1) for the quintessence models and in Fig. (2) for the phantom models.

For each potential, we investigate whether a change in one of the parameters or a change in the initial conditions can give the maximum range of the EOS parameter values, provided that the remaining parameters are fixed. We



The phantom potentials	BIC	AIC	Bayes factor
$V(\phi) = V_0\phi^2$	18.7	10	0.022
$V(\phi) = V_0(1 - \exp(\phi^2/\sigma^2))$	22.4	12	0.0049
$V(\phi) = V_0(1 - \cos(\phi/\kappa))$	22.4	12	0.0019
$V(\phi) = V_0(\cosh(\psi\phi))^{-1}$	22.4	12	0.0018
$V(\phi) = V_0\phi^5$	18.7	10	0.016
$V(\phi) = V_0\phi^{-2}$	18.7	10	0.0054
$V(\phi) = V_0 \exp(\beta\phi)$	22.4	12	0.017

TABLE IV: The list of the dark energy phantom potentials, with corresponding *BIC*, *AIC*, and Bayes factor values.

find that the dark energy potentials can be divided in two types. For the first type of the potentials, the change of the initial conditions only (the model parameters are fixed). The following quintessence potentials belong to this type: the RP, the ZWS, the Sahni-Wang and the phantom potentials: the quadratic, the Gaussian, the fifth power, the inverse square. In the second type of potentials, the change in one of the parameters only (another parameters and initial conditions are fixed) affect the maximum variation of the EOS parameter. The following quintessence potentials belong to the second type: the Sugra, the Ur̃ena-López-Matos, the Albrecht-Skordis, the Chang-Scherrer, the Barreiro-Copeland-Nunes and the phantom potentials: the pNGb, the inverse hyperbolic cosine, the exponent.

The contours in Figs. (1-2) represent 1, 2, and 3 $\sigma$  confidence levels for the CPL parametrization derived by fitting the same  $H(z)$ ,  $d_A(z)$ , and  $f\sigma_8$  data. All dark energy models include the  $\Lambda$ CDM value of  $w_0 = -1$ ,  $w_a = 0$ ,  $\gamma = 0.55$  as one of their limits.

## V. CONCLUSIONS

We have derived projected constraints on a number of dark energy models by fitting them to a mock  $H(z)$ ,  $d_A(z)$ ,  $f\sigma_8(z)$  data generated in a fiducial  $\Lambda$ CDM model.

Figs. (3-4) and (5) show examples of the constraints that we get for the quintessence RP, the Sahni-Wang potentials and for the phantom inverse hyperbolic cosine potential. Since all models have the  $\Lambda$ CDM model as their limit, strictly speaking it is impossible to rule them out based on the likelihood arguments alone. Therefore we also look at commonly cited model comparison criteria in the Bayesian statistics such as the Bayes factor, the *BIC* and *AIC* information criteria. Computing *BIC* and *AIC* in our setup is straightforward. Since all models have the same maximum likelihood by the construction the *BIC* and the *AIC* become simply functions of the number of the extra parameters. To compute the Bayes factor we integrated the posterior within the bounds given in the Tables I and II. The results of the *BIC*, *AIC*, and Bayes factors for all the dark energy models are summarized in the Tables III and IV. These numbers clearly demonstrated that if the  $\Lambda$ CDM model is the true description of dark energy, the full DESI data will be able to strongly discriminate most scalar field dark energy models currently under consideration.

These results however need to be taken with a grain of salt. The evidence values are very sensitive to the prior ranges. We only restricted the prior range based on constraints, by using the method developed by us. Further restriction of the parameter ranges could significantly increase the evidence value. The results were derived assuming a fiducial  $\Lambda$ CDM model and the low value of evidence simply means that the model would be easier to discriminate if  $\Lambda$ CDM were the true model. The flip side of this is that if instead the dynamic dark energy models were true that would also show up more obviously in the data.

We also explored how the dark energy models are mapped to the CPL parameter surface. For the models considered in our work this parametrization seems to work reasonably well even for the wide redshift range.

## Acknowledgments

It is our great pleasure to thank Bharat Ratra for useful comments and discussions. We appreciate discussions with Natalia Arhipova, Leonardo Campanelli, Vasil Kukhianidze, Olga Navros, and Alexander Tevzadze. Support through the Shota Rustaveli Georgian NSF (grants FR/339/6-350/14 and PhD\_F\_17\_196), the CRDF-SRNSF-GRDF Georgia

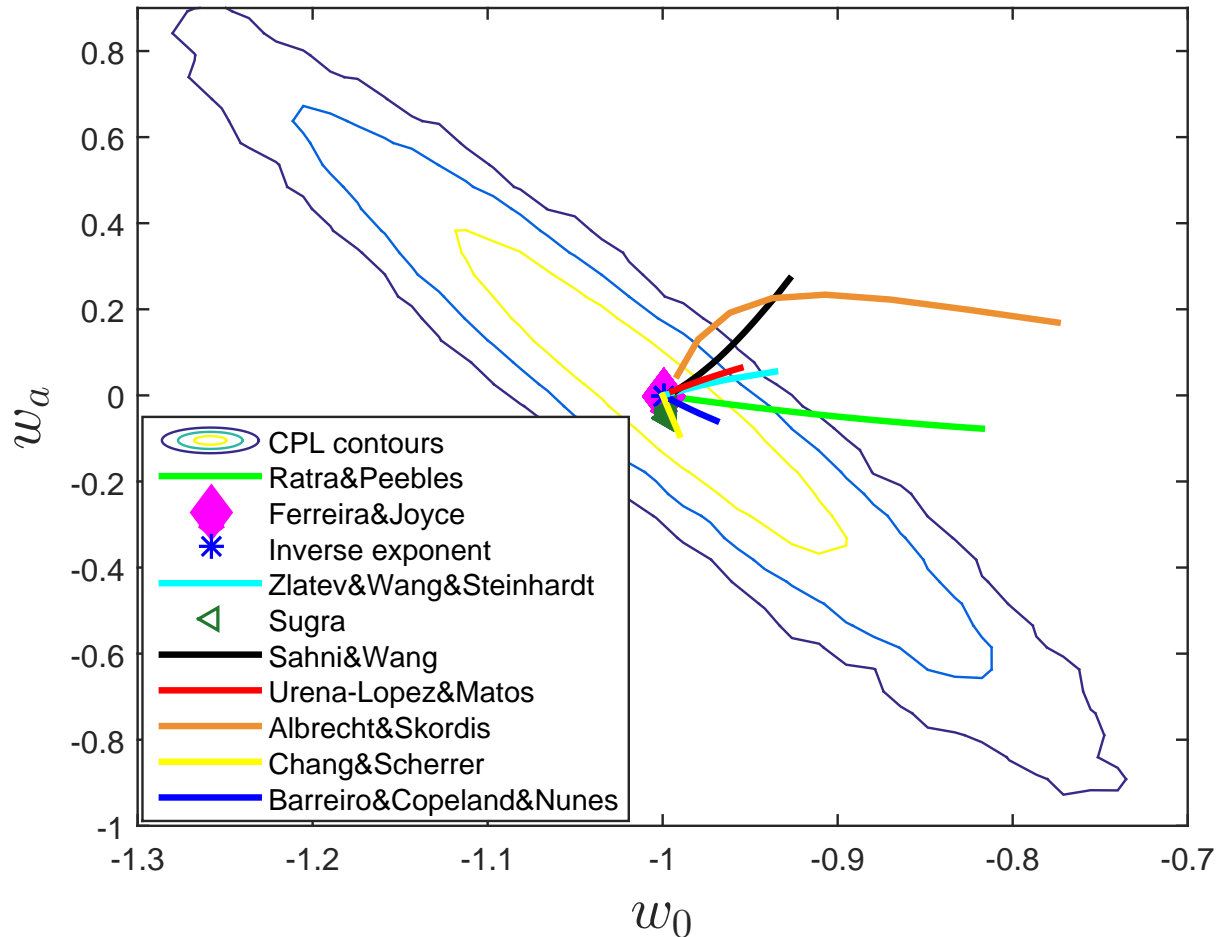


FIG. 1: The comparison of the possible  $(w_0, w_a)$  values of the quintessence dark energy potentials with the CPL- $\Lambda$ CDM  $3\sigma$  confidence level contours.

Women's Research Fellowship Program grant WRF-14-22, the Swiss NSF SCOPES (grant IZ7370-152581), and the NSF Astrophysics and Astronomy Grant (AAG) Program (grant AST1615940), DOE grant DEFG 03-99EP41093, and NASA grant 12-EUCLID11-0004 are gratefully acknowledged. TK also thanks the High Energy and Cosmology division and the Associate Membership Program at International Center for Theoretical Physics (ICTP) for hospitality and partial support.

- 
- [1] A. G. Riess et al. (Supernova Search Team), *Astron. J.* **116**, 1009 (1998).  
[2] S. Perlmutter et al. (Supernova Cosmology Project), *Astrophys. J.* **517**, 565 (1999).  
[3] E. Komatsu and WMAP Cosmology Project, *Astrophys. J.* **192**, 18 (2011).  
[4] J. Frieman, M. Turner, and D. Huterer, *Ann. Rev. Astron. Astrophys.* **46**, 385 (2008).  
[5] D. H. Weinberg, M. J. Mortonson, D. J. Eisenstein, C. Hirata, A. G. Riess, and R. E., *Phys. Rept.* **530**, 87 (2013).  
[6] S. M. Carroll, *Living Rev. Rel.* **4**, 1 (2001).  
[7] V. Sahni, *Class. Quant. Grav.* **19**, 3435 (2002).  
[8] T. Padmanabhan, *Phys. Rept.* **380**, 235 (2003).  
[9] P. J. E. Peebles and B. Ratra, *Rev. Mod. Phys.* **75**, 559 (2003).  
[10] J. Martin, *Comptes Rendus Physique* **13**, 566 (2012).  
[11] A. Padilla, 1502.05296 (2015).



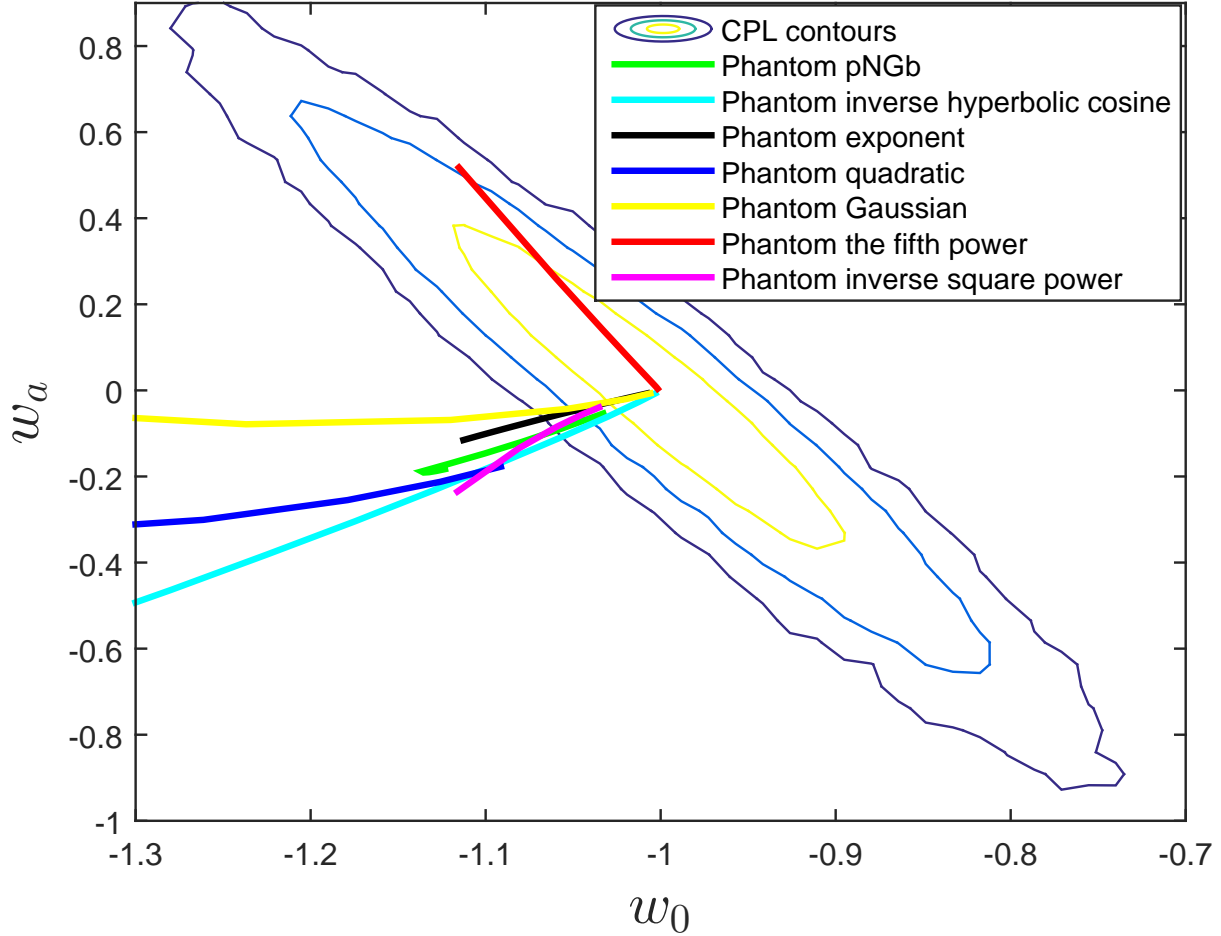


FIG. 2: Similar to the Fig. (2), for the phantom models.

- [12] E. J. Copeland, M. Sami, and S. Tsujikawa, *Int. J. Mod. Phys. D* **15**, 1753 (2006).
- [13] R. R. Caldwell and M. Kamionkowski, *Ann. Rev. Nucl. Part. Sci.* **59**, 397 (2009).
- [14] B. Ratra and P. J. E. Peebles, *Phys. Rev. D* **37**, 3406 (1988).
- [15] P. J. Steinhardt, L.-M. Wang, and I. Zlatev, *Phys. Rev. D* **59**, 123504 (1999).
- [16] R. R. Caldwell and P. J. Steinhardt, *Phys. Rev. D* **57**, 6057 (1998).
- [17] I. Zlatev, L.-M. Wang, and P. J. Steinhardt, *Phys. Rev. Lett.* **82**, 896 (1999).
- [18] R. R. Caldwell and E. V. Linder, *Phys. Rev. Lett.* **95**, 141301 (2005).
- [19] E. V. Linder, *Gen. Rel. Grav.* **40**, 329 (2008).
- [20] K. J. Ludwick, *Mod. Phys. Lett. A* **32**, 1730025 (2017).
- [21] P. G. Ferreira and M. Joyce, *Phys. Rev. D* **58**, 023503 (1998).
- [22] P. Brax and J. Martin, *Phys. Lett. B* **468**, 40 (1999).
- [23] V. Sahni and L.-M. Wang, *Phys. Rev. D* **62**, 103517 (2000).
- [24] L. A. Urena-Lopez and T. Matos, *Phys. Rev. D* **62**, 081302 (2000).
- [25] A. Albrecht and C. Skordis, *Phys. Rev. Lett.* **84**, 2076 (2000).
- [26] H.-Y. Chang and R. J. Scherrer 1608.03291 (2016).
- [27] T. Barreiro, E. J. Copeland, and N. J. Nunes, *Phys. Rev. D* **61**, 127301 (2000).
- [28] S. Dutta and R. J. Scherrer, *Phys. Lett. B* **676**, 12 (2009).
- [29] J. A. Frieman, C. T. Hill, A. Stebbins, and I. Waga, *Phys. Rev. Lett.* **75**, 2077 (1995).
- [30] R. Rakhi and K. Indulekha 0910.5406 (2009).
- [31] R. J. Scherrer and A. A. Sen, *Phys. Rev. D* **78**, 067303 (2008).
- [32] N. Suzuki and T. Supernova Cosmology Project, *Astrophys. J.* **746**, 85 (2012).
- [33] M. Betoule et al. (SDSS), *Astron. Astrophys.* **568**, A22 (2014).

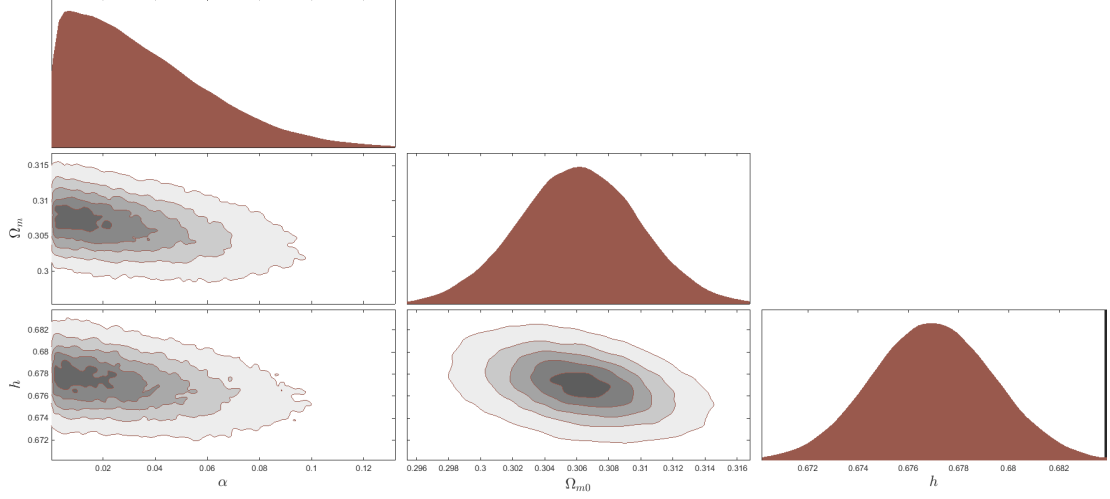


FIG. 3: The confidence-level contour plots for various pairs of the free parameters ( $\alpha$ ,  $\Omega_{m0}$ ,  $h$ ) for which the  $\phi$ CDM model with the Ratra-Peebles potential  $V(\phi) = V_0 M_{pl}^2 \phi^{-\alpha}$  is in the best fit with the  $\Lambda$ CDM model.

- [34] P. A. R. Ade et al. (Planck), *Astron. Astrophys.* **571**, A16 (2014).
- [35] P. A. R. Ade et al. (Planck 2015 results. XIII. Cosmological parameters), *Astron. Astrophys.* (2015).
- [36] A. Heavens, Y. Fantaye, E. Sellentin, H. Eggers, Z. Hosenie, S. Kroon, and A. Mootoivaloo, *Phys. Rev. Lett.* **119**, 101301 (2017).
- [37] S. Dhawan, A. Goobar, E. Mrtzell, R. Amanullah, and U. Feindt, *JCAP* **1707**, 040 (2017).
- [38] A. I. Lonappan, S. Kumar, Ruchika, B. R. Dinda, and A. A. Sen (2017).
- [39] A. Font-Ribera, P. McDonald, N. Mostek, B. A. Reid, H.-J. Seo, and A. Slosar, *JCAP* **1405**, 023 (2014).
- [40] M. Levi et al. (DESI) (2013), 1308.0847.
- [41] A. Aghamousa et al. (DESI) (2016), 1611.00036.
- [42] J. Kwan *et al.* [DES Collaboration], *Mon. Not. Roy. Astron. Soc.* **464**, no. 4, 4045 (2017).
- [43] L. Amendola *et al.* [Euclid Theory Working Group], *Living Rev. Rel.* **16**, 6 (2013).
- [44] D. Spergel et al., 1503.03757 (2015).
- [45] M. Chevallier and D. Polarski, *Int. J. Mod. Phys.* **D10**, 213 (2001).
- [46] E. V. Linder, *Phys. Rev. Lett.* **90**, 091301 (2003).
- [47] L.-M. Wang and P. J. Steinhardt, *Astrophys. J.* **508**, 483 (1998).
- [48] P. Wu, H. W. Yu, and X. Fu, *JCAP* **0906**, 019 (2009).
- [49] E. V. Linder, *Phys. Rev.* **D72**, 043529 (2005).
- [50] O. Avsajanishvili, N. A. Arkhipova, L. Samushia, and T. Kahniashvili, *Eur. Phys. J.* **C74**, 3127 (2014).
- [51] O. Avsajanishvili, L. Samushia, N. A. Arkhipova, and T. Kahniashvili, in *5th Gamow International Conference in Odessa: "Astrophysics and Cosmology after Gamow: progress and perspectives"* Odessa, Ukraine, August 16-23, 2015.
- [52] B. Ratra and P. J. E. Peebles, *Astrophys. J.* **325**, L17 (1988).

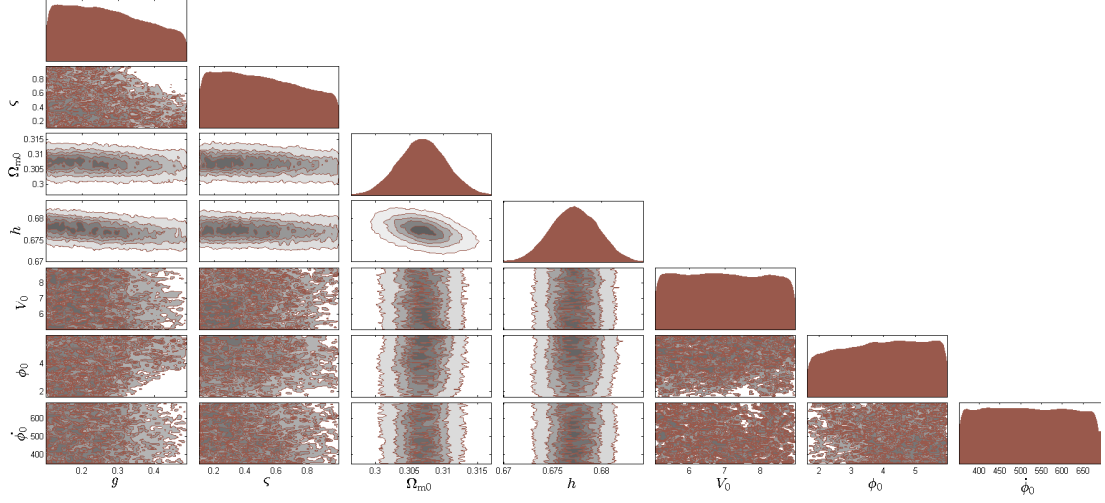


FIG. 4: The confidence-level contour plots for various pairs of the free parameters  $(g, \varsigma, \Omega_{m0}, h, V_0, \phi_0, \dot{\phi}_0)$  for which the  $\phi$ CDM model with the Sahni-Wang potential  $V(\phi) = V_0(\cosh(\varsigma\phi) - 1)^g$  is in the best fit with the  $\Lambda$ CDM model.

[53] M. O. Farooq, Ph.D. thesis, Kansas State U. (2013).

[54] H. Akaike, IEEE Transactions on Automatic Control **19**, 716723 (1974).

[55] L. Samushia, Ph.D. thesis, Proquest Dissertations And Theses 2009. Section 0100, Part 0606 107 pages; [Ph.D. dissertation].United States – Kansas: Kansas State University; 2009. Publication Number: AAT 3380411. Source: DAI-B 70/12, Jun 2010 (2009).

[56] G. E. Schwarz, Annals of Statistics **06**, 461464 (1978).

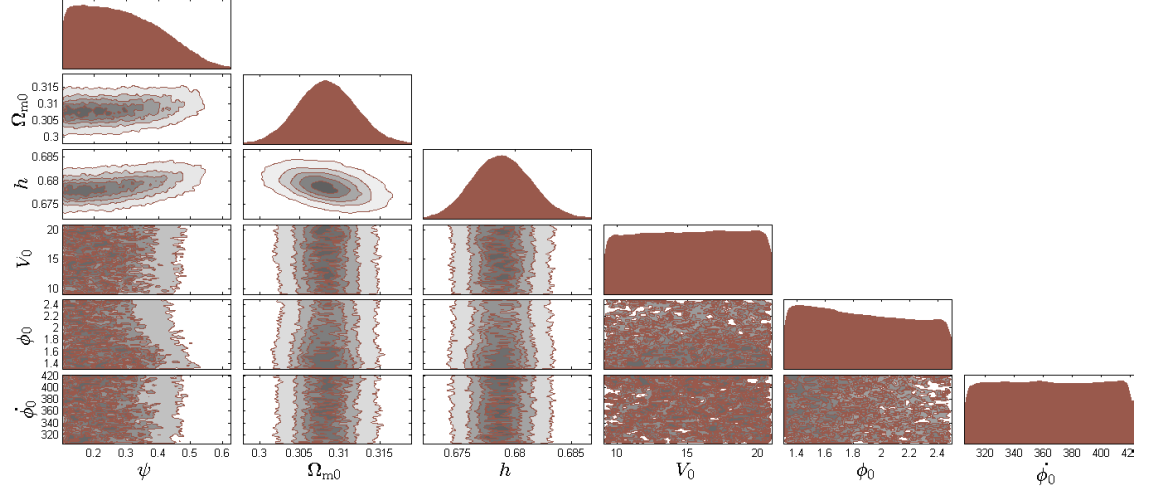


FIG. 5: The confidence-level contour plots for various pairs of the free parameters  $(\psi, \Omega_{m0}, h, V_0, \phi_0, \dot{\phi}_0)$  for which the  $\phi$ CDM model with the phantom inverse hyperbolic cosine potential  $V(\phi) = V_0(\cosh(\psi\phi))^{-1}$  is in the best fit with the  $\Lambda$ CDM model.